# Relating Underlying Performance Objectives of Overground Walking to Observable Walking Mechanics using Predictive Musculoskeletal Simulations

Wentao Li and Nicholas P. Fey, Member, IEEE

Abstract— There exists motor redundancy during human gait that allows individuals to perform the same task in different observable ways (i.e., with varied styles). However, how differences in observable walking mechanics depend on unique and underlying biomechanical objectives is unclear. As an example, these objectives could include metabolic energy consumption, sum of muscle activations, limb mechanical loading, balance and combinations thereof. In this study, we develop predictive neuromuscular simulations to investigate the relationships between these biomechanical objectives and observable mechanics during level walking. We simulated 3D normal walking of five healthy subjects, while optimizing each of the aforementioned objectives-resulting in 25 forward dynamics simulations for analysis. We compared the resulting joint kinematics and moments of different simulations. One of main findings suggests that decreased hip abduction angle is tightly related to when the regulation of dynamic balance (computed as whole-body angular momentum) is included in a movement cost function. We also find that increased joint moments are related to including metabolic cost (i.e., objectives associated with improving the energy economy of movement). Further, the timing of joint kinematics is adjusted for different performance objectives. These findings could guide the development of rehabilitation training and assistive devices that target specific individuals, tasks, and specific styles of movement.

### I. INTRODUCTION

Human gait is complex, and one can perform a specific movement task in varied and preferred styles. These variabilities, resulting from the intrinsic redundancy of human neuro-musculoskeletal system and the subject-specific anthropometric characteristics enable us to better adapt to complicated environments. In rehabilitation and assistive engineering, it is important to provide the affected individual with opportunities to fully and effectively participate in varying functions of daily life. For instance, intent-recognition and task-dependent algorithms were developed for intelligent lower-limb prosthesis to provide users with increased adaptability to different tasks [1]. However, there could be high-level biomechanical performance objectives associated with different locomotion tasks that contribute to specific walking style choices. Therefore, understanding how one could mediate walking styles (i.e., observable walking mechanics) for different performance objectives is significant for the development of rehabilitation training and assistive

Several biomechanical objectives could be related to the different walking styles. Balance is an essential consideration during human walking, and may significantly affect the mechanics of gait. Healthy adults make preparatory and response-based adjustments to dynamic balance based on walking styles during 45 degree turns [2], and individuals with Parkinson's disease experience increased difficulties maintaining forward balance during stair ambulation [3]. Although balance regulation is critical, there are other performance objectives that are important during walking. For example, human walking speed selection is related to minimum metabolic energy cost per unit distance traveled [4], which was thought to be continuously optimized in human walking [5]. Meanwhile, musculoskeletal simulations of human gait suggest that minimizing muscle effort or fatigue may be also a governing principle of human walking because optimization of total muscle activation produced gait with realistic knee flexion [6]. These objectives are particularly useful in sedentary populations, and simulations using fatigue-related objectives successfully predict the higher metabolic energy consumption, lower walking speed, altered hip and ankle kinematics of the elderly [7]. Furthermore, lower-limb loading is another biomechanical factor in human walking that would be important, especially in populations with lower-limb amputation that frequently develop joint diseases like osteoarthritis and osteoporosis [8].

Recently, researchers have used empirical and simulation approaches to study the gait mechanics in relation to the underlying biomechanical objectives of human locomotion. For instance, many studies investigated the balance/stability regulation strategies and associated different mechanics during gait through experiment [9], [10]. Antos et al., explored the relationship between step length-width choices and metabolic energy expenditure through measuring metabolic power for two-alternative forced-choice walking paradigm, and found that longer steps with higher energy expenditures were preferred over shorter and wider steps [11]. Miller et al., investigated the preferred performance objective in human running through 2D musculoskeletal simulations and suggested that minimizing muscle activation produced more realistic and economical running [12]. Recently, Veerkamp et al., used two-dimensional musculoskeletal model with reflex control paradigms to show that optimizing various

devices that adapt to individual and context.

<sup>\*</sup> This work was support by grants from the Mobility Foundation Center for Rehabilitation Research and the National Science Foundation, National Robotics Initiative Grant #2054343.

W. Li, is with the Walker Department of Mechanical Engineering at the Cockrell School, University of Texas at Austin, Austin, TX 78712 USA (e-mail: wentao.li@utexas.edu).

N. P. Fey is with the Walker Department of Mechanical Engineering at the Cockrell School, University of Texas at Austin, Austin, TX 78712 USA (e-mail: nfey@utexas.edu).

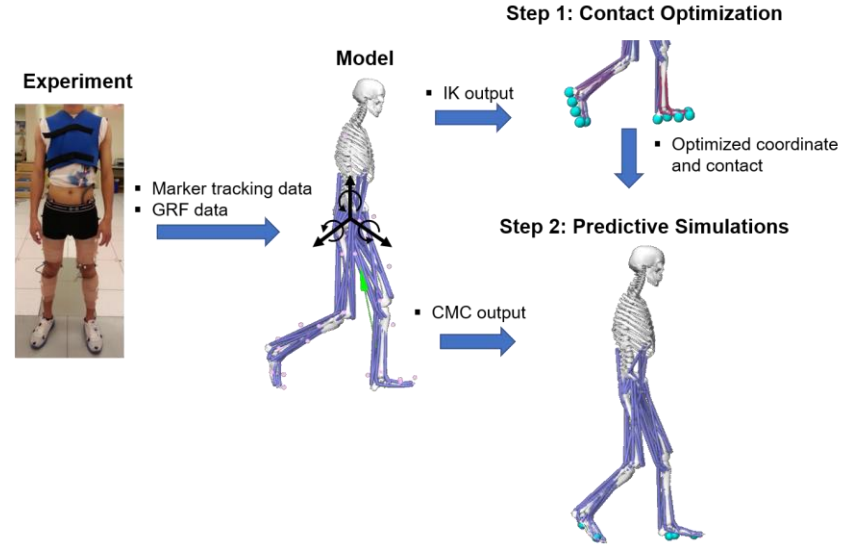


Fig. 1. Diagram of the two-step simulation framework. Static marker tracking data from experiment were used to build subject-specific musculoskeletal models that consists of 21 DOF and 92 muscle-tendon actuators. Gait marker tracking data and GRF data from experiment were then used to perform inverse kinematics (IK) and computed muscle control (CMC) analyses in OpenSim that produced joint kinematics and muscle dynamics, respectively. Resulting joint kinematics and experiment GRF data were considered to be more accurate, and were used to optimize foot-ground contact model parameters in the Step 1 simulation. Resulting contact model parameters were used for the predictive simulations of Step 2, and CMC results were used as initial guess of muscle-tendon actuator dynamics for the optimization.

optimization objectives, including energy expenditure, muscle activations, head stability, derivatives of ground reaction forces (GRF) and knee extension produces realistic gait [13]. Similarly, many other simulations of human locomotion by minimizing multiple biomechanical objectives together produced results that have relatively agreed with gait experiment data [14], [15]. However, there is still little understanding on the relationship between the observable walking mechanics and different biomechanical performance objectives.

Therefore, in this study we performed predictive neuromusculoskeletal simulations of human walking by optimizing specific performance objectives, and compared joint angles and moments (i.e., biomechanical metrics that can be observed/quantified relatively easily in human participants) of each simulation to investigate the relationship between biomechanical objectives and walking mechanics. Understanding these relationships between observable walking mechanics and specific performance objectives could guide the development of rehabilitation training and assistive devices that target specific individuals, tasks, and specific styles of movement. This predictive analysis can specify how the actuation and/or coordination of specific lower-extremity joints, and their degrees-of-freedom, mediate changes in movement style. We expect that new device and training interventions could target not only specific tasks (such as walking), but to do so with an increased resolution that incorporates movement style.

### II. METHODS

### A. Experiment

Subject-specific tracking data for this study was provided by a prior experiment [2], [16] of five able-bodied subjects performing level straight walking at their preferred walking speeds. All participants provided written informed consent to participate in the experiment that was approved by the Institutional Review Board. A 10-camera motion capture system (Motion Lab Systems, Inc.) operating at 120 Hz was used to record motion trajectories of 42 reflective markers attached on human body. Ground reaction forces were recorded by six force plates operating at 1200 Hz. Recorded data were processed in Visual3D (C-Motion, Inc.) and OpenSim [17].

## B. Musculoskeletal Model and Simulation Framework

We built a musculoskeletal model for each subject in OpenSim by scaling an generic model [18] and minimizing the tracking errors of reflective markers in static poses. Each model had 21 degrees of freedom (DOF) with metatarsophalangeal joint locked, and was actuated by

92 Hill-type muscle-tendon actuators. Inverse kinematics (IK) and computed muscle control (CMC) analyses were performed for a walking trial of each subject to obtain experimental joint kinematics and muscle dynamics.

The simulation framework of this study was revised from our previous research [19]. Each simulation was formulated as an optimal control problem, as in

$$\min_{\mathbf{r}, \mathbf{u}} J \tag{1-a}$$

Subject to: 
$$\dot{\mathbf{x}} = f(\mathbf{x}, \mathbf{u}, t)$$
 (1-b)

$$x_{lb} \le x(t) \le x_{ub} \tag{1-c}$$

$$\mathbf{u}_{lb} \le \mathbf{u}(t) \le \mathbf{u}_{ub} \tag{1-d}$$

where x is the state vector, including joint angles, joint angular velocities, muscle fiber length, and muscle activations; u is the control vector, i.e., muscle excitations;  $x_{lb}$  and  $x_{ub}$  are the lower and upper bound of the state variables;  $u_{lb}$  and  $u_{ub}$  are the lower and upper bound of the control variables; the state space equation represents the dynamics of the musculoskeletal model. The optimal control problem (1a-d) were solved using direct collocation, and were transformed to a large-scale nonlinear optimization problem [20]. Customized MATLAB (Mathworks, Inc.) code was written to solve the nonlinear optimization problem.

The foot-ground contact was modeled as smoothed Hunt-Crossley force [21] between 12 spheres under each foot and a half-space representing the flat ground. For each subject, the first step of a two-step simulation framework (Fig. 1) was contact-optimization simulation aimed to optimize locations of contact spheres and contact model parameters to track the experimental ground reaction forces and joint kinematics. In

this step, the optimization variables were discretized joint angles and angular velocities, and the objective function was the tracking errors of the resulting ground reaction forces relative to the experimental GRFs as well as the errors between optimization variables and IK results. Using the optimized contact model parameters, the second-step simulations were then performed, including a metabolic-based simulation, a balance-based simulation, a muscle-effort-based simulation, a loading-based simulation and a multi-objective simulation

The metabolic-based simulation used an objective function with a metabolic energy term and a GRF penalty term (Eq. 2). The total metabolic energy was calculated as summation of the time integral of the net metabolic energy rate  $\dot{E}$  of each muscle [22]. The penalty term P was a function of simulated GRF and contact force between right and left ankles that aimed to avoid unrealistic large or small vertical GRF (the first two terms where relu refers to rectified linear unit function), encourage smooth GRF trajectories (the third term), and avoid interferences between limbs (Eq. 3). This GRF penalty term existed in every second-step simulation objective function.

$$J_{1} = \int_{0}^{t_{f}} \left( w_{1} \frac{1}{Step \ Length * BW} \left\| \dot{E} \right\|_{2}^{2} + w_{2} P \right) dt. \tag{2}$$

$$\begin{split} P &= \int_0^{t_f} \left( w_1 * relu \left( LB - \frac{GRF_y}{BW} \right)^2 + w_2 * relu \left( \frac{GRF_y}{BW} - UB \right)^2 + \right. \\ &\left. w_3 \left( \frac{d^2 GRF}{dt^2} \right)^2 + w_4 \|F_c\|_2^2 \right) dt \,. \end{split} \tag{3}$$

The balance-based simulation used an objective function minimizing normalized whole-body angular momentum (H) about the body's center-of-mass that is a measure of dynamic balance with smaller value indicating tighter regulation of dynamic balance [2], [19], as in:

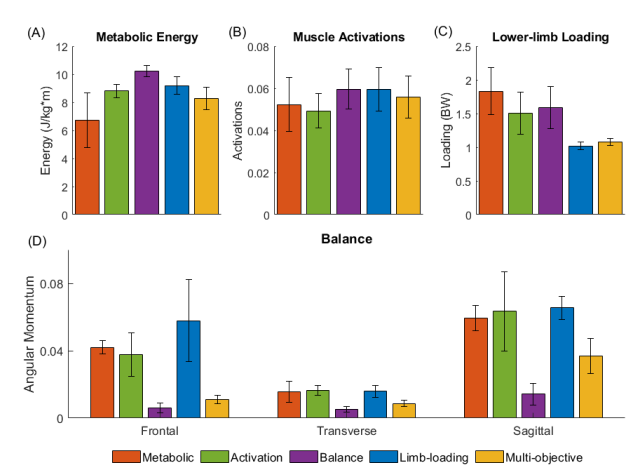


Fig. 2. Mean and one standard deviation of resulting biomechanical performances of each simulation, i.e., (A) normalized metabolic energy, (B) normalized sum of muscle activations, (C) maximum lower-limb loading, and (D) range of 3D normalized whole-body angular momentum (H), a measure of dynamic balance.

$$J_2 = \int_0^{t_f} (w_1 ||H||_2^2 + w_2 P) dt. \tag{4}$$

The muscle-effort or activation-based simulation used an objective function that minimized the summation of the time integral of muscle activation level a of all muscles, as in:

$$J_3 = \int_0^{t_f} (w_1 ||a||_2^2 + w_2 P) dt.$$
 (5)

The loading-based simulation minimized the maximum of simulated vertical GRF that was approximated as in:

$$J_4 = \frac{w_1}{BodyWeight} \log \left( \sum \exp \left( \frac{GRF_{vertical}}{constant} \right) \right) + w_2 \int_0^{t_f} P dt.$$
 (6)

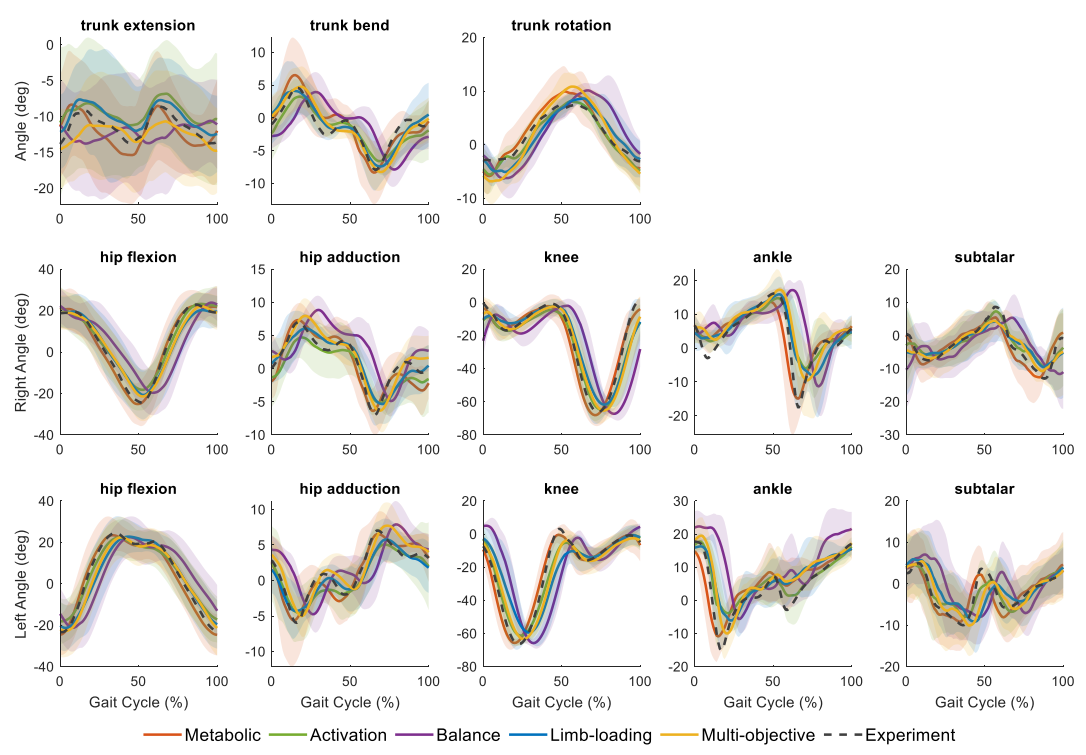


Fig 3. Mean (solid lines) and one standard deviation (shaded areas) of resulting joint angles of metabolic-energy, muscle-activation, dynamic-balance, limb-loading, multi-objective-based simulations and experiment mean. Top, middle and bottom rows are joint angles of trunk, right limb and left limb, respectively. The data shown were from right heel-strike (0% gait cycle) to right heel-strike (100% gait cycle).

The objective function of multi-objective simulation includes all of the four above-mentioned biomechanical objectives, as in:

$$J_5 = J_1 + J_2 + J_3 + J_4. (7)$$

Collectively, we randomly selected one trial from each subject, and optimized this trial for each of the five aforementioned performance objects. 25 predictive simulations in total were performed. For each simulation, periodic constraints were applied to each simulation so that the coordinates or joint angles at initial time equal those at final time. After predictive simulations, we analyzed the resultant data from right-leg toe-off to toe-off. Inverse Dynamics analyses were performed in OpenSim to obtain the resulting joint moments.

### C. Statistical Analysis

The magnitude and timing of peak joint angles, maximum and minimum joint moments were compared among different simulations as well as experiment using one-way repeated measures ANOVA ( $\alpha$ =0.05). *Post-hoc* comparisons were performed using Tukey-Kramer's criterion.

#### III. RESULTS

The first-step simulation optimized contact model parameters, and produced experiment-matched GRFs and joint kinematics that matched IK results. The second-step predictive simulation resulted in increased biomechanical performances for each simulation (Fig. 2).

The timing of peak kinematics (Fig. 3) of balance-based simulation was leading for trunk extension relative to multiobjective simulation (p = 0.042, 95% CI: 1.30 - 51.90% gait cycle) and experiment (p = 0.032, CI: 2.15 – 31.85%), and was lagging in trunk bending relative to all but activation-based simulations and experiment (p < 0.035, CI: 1.16 – 24.27%), in trunk rotation relative to metabolic-based simulation (p =0.021, CI: 2.53 - 19.87%), in right hip extension relative to experiment (p = 0.035, CI: 1.03 - 19.37%), in right hip adduction compared with metabolic, multi-objective simulations and experiment (p < 0.026, CI: 1.29 – 22.64%), in right hip abduction relative to multi-objective simulations and experiment (p < 0.044, CI: 0.31 – 19.92%), in right ankle plantarflexion relative to experiment (p = 0.024, CI: 2.28 – 20.92%), in right subtalar inversion compared with metabolic, multi-objective simulation and experiment (p < 0.048, CI: 0.095 - 15.51%), in left hip adduction compared to metabolic, multi-objective simulations and experiment (p < 0.032, CI: 1.19 - 25.07%), in left hip abduction compared to experiment (p < 0.019, CI: 2.50 - 17.50%), in left ankle plantarflexion relative to experiment (p = 0.015, CI: 3.35 – 19.05%), and in left subtalar eversion compared with activation-based simulation and experiment (p < 0.021, CI: 2.52 – 19.48%).

The peak trunk counter-clockwise rotation angle was larger in multi-objective simulation compared with experiment (p = 0.017, CI: 0.94 - 6.17). The peak right hip extension angle reduced in loading-based simulation relative to experiment (p = 0.037, CI: 0.18 - 4.13). The peak right hip abduction angle decreased in balance-based simulation compared with experiment (p = 0.041, CI: 0.14 - 4.30). The peak right plantarflexion angle reduced in balance-based simulation relative to metabolic-based simulation (p = 0.045, CI: 0.14 - 9.00) and experiment (p = 0.008, CI: 2.47 - 9.49). The right subtalar inversion angle reduced in activation-based (p = 0.020, CI: 0.58 - 4.53) and multi-objective simulation (p = 0.020, CI: 0.58 - 4.53) and multi-objective simulation (p = 0.020, CI: 0.58 - 4.53)

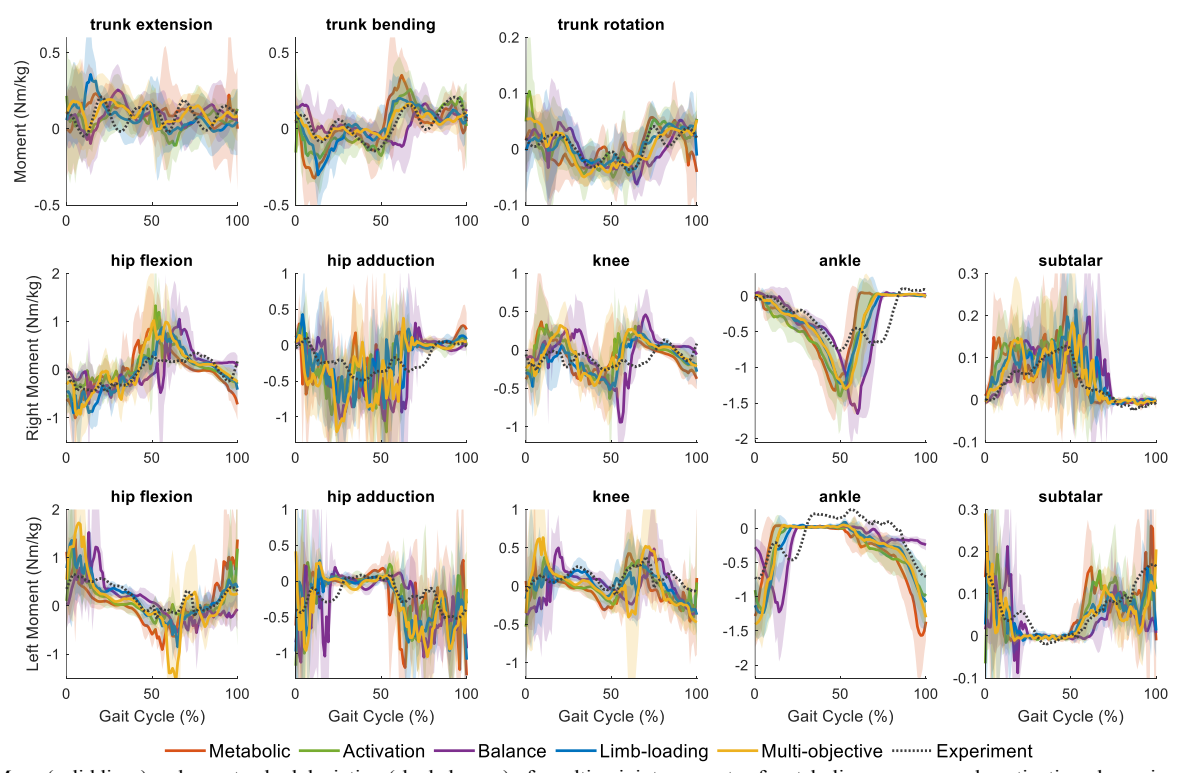


Fig 4. Mean (solid lines) and one standard deviation (shaded areas) of resulting joint moments of metabolic-energy, muscle-activation, dynamic-balance, limb-loading, multi-objective-based simulations and experiment mean. Top, middle and bottom rows are joint moments of trunk, right limb and left limb, respectively.

= 0.029, CI: 0.38 - 4.62) compared with experiment. The peak left subtalar inversion angle increased in balance-based simulation compared to multi-objective simulation (p = 0.049, CI: 0.007 - 2.70).

The maximum trunk right bending moment increased in activation-based simulation relative to multi-objective simulation (p = 0.044, CI: 0.0046 - 0.25). The maximum right hip adduction moment was larger in metabolic, activation and load-based simulations than experiment (p < 0.046, CI: 0.030 -2.09), and decreased in activation-based simulation relative to load-based simulation (p = 0.008, CI: 0.18 - 0.68). The maximum right hip abduction moment increased in metabolicbased simulation compared with load-based simulation and experiment (p < 0.021, CI: 0.26 - 2.40), and increased in multiobjective simulation relative to experiment (p = 0.012, CI: 0.44 -0.68). The maximum left hip adduction moment was greater in balance-based simulation than experiment (p = 0.022, CI: 0.28 - 2.37), and the maximum left hip abduction moment increased in all simulations except metabolic compared with experiment (p < 0.017, CI: 0.31 – 2.51). The maximum right knee extension moment increased in balance and multiobjective simulation relative to experiment (p < 0.044, CI: 0.021 - 1.02). The maximum left subtalar inversion moment was larger in metabolic and load-based simulation than experiment (p < 0.044, CI: 0.0080 - 0.44).

### IV. DISCUSSION

In this study, we performed predictive simulations of normal human walking using dynamic optimization and direct collocation approaches. Different biomechanical performance metrics were used as optimization objective functions to investigate the variations of human walking styles, i.e., observable kinematics and joint kinetics, associated with these biomechanical objectives. The targeted performances, i.e., metabolic energy cost, sum of muscle activations, lower-limb loading (measured as maximum vertical GRF) and balance regulation (measured by whole-body angular momentum)

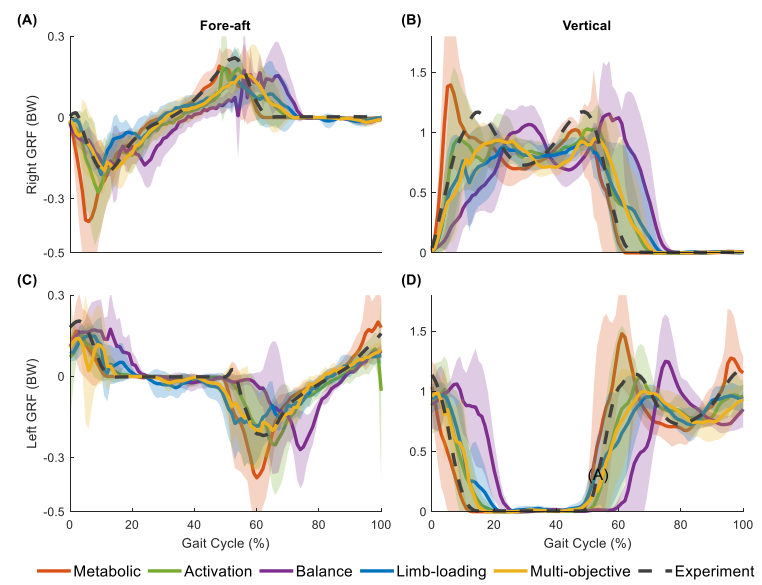


Fig. 5. Mean (solid lines) and one standard deviation (shaded areas) of the trajectories of resulting fore-aft and vertical ground reaction forces of metabolic-energy, muscleactivation, dynamic-balance, limb-loading, multi-objective-based simulations and experiment mean. GRFs in mediolateral direction were small and not shown in this figure.

were improved in each simulation, and associated joint kinematic and kinetic changes were observed.

During balance-based simulation dynamic balance was more tightly regulated, with reduced range of whole-body angular momentum (Fig. 2C), which was achieved through adjusting specific joint kinematics. During swing phase the right hip abduction angle significantly decreased in balancebased simulation relative to experiment (Fig. 3). While not statistically significant, during single-leg stance phase the right hip adduction angle increased in balance-based simulation compared to other simulations as well as experiment for each subject (Fig. 3 shows average). This adjustment could be a strategy to maintain mediolateral balance during gait. Individuals may translate the horizontal projection of body center of mass (CM) to fall into the base of support through modifying hip adduction/abduction angle, and thus, increase walking balance. Another explanation of the adjustment to stance-leg hip adduction could be related to centroidal moment pivot (CMP), the point where a line parallel to the ground reaction force, passing through the CM, intersects with the ground [23]. This movement could translate the center of pressure (CP) position towards and coincide with CMP, and therefore, decrease horizontal moments about CM as well as whole-body angular momentum. Furthermore, these adjusted right hip adduction kinematics did not increase the maximum moment of associated joints (Fig. 4), which may suggest it as a potential strategy for strictly regulating dynamic balance that does not require high joint loading. These findings of adjusted hip adduction for more balanced walking may also suggest that future assistive devices should target at not only the ankle joint but also the hip joint for enhanced balance assistance. Furthermore, the reduced right plantarflexion angles (Fig. 3) in balance-based simulations may suggest less dependence of dynamic balance on increased plantarflexion that many currently-available assistive technologies are trying to produce with active push-off. However, future work is needed to further investigate the mechanics of amputee walking to determine the effects of such joint kinematics.

> In metabolic-based simulation, peak hip extension tended to increase near contralateral heel-strike (Fig. 3), while not statistically significant. This may be related to the objective function of metabolic-based simulations (Eq. 2) that normalizes cost of transport (CoT) by step length. With increased contralateral hip extension at heel-strike, the model could increase step length and thus, decrease CoT. However, this strategy of minimizing CoT may be at cost. Lower-limb loading or vertical GRFs were higher in metabolic-based simulations relative to other simulations (Fig. 2B, Fig. 5). In contrast to the aggressive movement adjustments and higher limb loadings of metabolic-based simulations, muscle-activation-based simulations produce similar metabolic energy and total muscle activations with lower limb loadings (Fig. 2A, B, C). Therefore, muscle activations may be a more realistic biomechanical objectives for human locomotion relative to metabolic-based objectives, which supports the conclusion of a previous study that suggests a potential control

strategy centered on muscle activations for economical running [12]. Furthermore, the maximum moment of right hip adduction, abduction and left subtalar inversion also increased in metabolic-based simulation relative to experiment (Fig. 4). Since hip adduction/abduction could contribute to balance regulation as discussed beforehand, it may require excessive effort to maintain balance to reduce metabolic energy cost in metabolic-based simulations.

Despite the magnitude, the timing of joint kinematics was also adjusted for different simulations. During balance-based simulations, there were phase lags of trunk and lower-limb movements compared to other simulations, such as trunk bending, trunk rotation, hip extension, hip adduction, abduction, ankle plantarflexion, and subtalar inversion (Fig. 3). This may be due to the elongated double support phase of balance-based simulations (Fig. 5), which has been thought to be beneficial for balance regulation during gait [24]. Furthermore, the elongated double support phase could provide more time for neuromuscular adjustments in preparation of single support phase that is more challenging in balance regulation. However, metabolic-based simulations tended to create leading phases of lower-limb movements relative to other simulations, such as hip flexion, knee angle, ankle angle and subtalar angle (Fig. 3). The timing of first peak vertical GRF of right (p = 0.035, CI: 0.92 - 14.68%) and left (p = 0.033, CI: 0.81 - 11.19%) leg during metabolic-based simulation was leading relative to experiment (Fig. 5 B, D). This movement strategy may lead to a shorter period of singleleg support phase that was found to represent the greatest percentage of total muscular energy cost [22]. Therefore, joint kinematic phasing of walking could be related to specific performance objectives, and may need to be targeted in the development of intelligent assistive devices.

In this study, we performed predictive simulations of human walking to investigate different walking mechanics that relate biomechanical objectives. Altered adduction/abduction angle during balance-based simulations could be related to tight regulation of dynamic balance. Increased joint moment is found in metabolic-based simulations, which may suggest greater effort to reduce metabolic energy cost. Furthermore, altered phasing of joint kinematics was found associated with specific performance objectives. These findings could guide the development of rehabilitation training and assistive devices that target specific individuals, tasks, and specific styles of movement. However, there are limitations within this study. The model of this study did not include arms or MTP joint, which could be important in specific gait functions. The results of the current study were produced by computer simulation and optimization algorithms and future study is needed to further assess these simulation results to investigate whether they are realistic.

### REFERENCES

- [1] H. A. Varol, F. Sup, and M. Goldfarb, "Multiclass Real-Time Intent Recognition of a Powered Lower Limb Prosthesis," *IEEE Trans. Biomed. Eng.*, vol. 57, no. 3, pp. 542–551, Mar. 2010.
- [2] W. Li, N. T. Pickle, and N. P. Fey, "Time evolution of frontal plane dynamic balance during locomotor transitions of altered anticipation and complexity," J. Neuroeng. Rehabil., vol. 17, no. 1, pp. 1–12, 2020.
- [3] W. Li and N. P. Fey, "Whole-body and Segmental Contributions to

- Dynamic Balance in Stair Ambulation are Sensitive to Early-Stage Parkinson's Disease," in 2021 43rd Annual International Conference of the IEEE Engineering in Medicine & Biology Society (EMBC), Nov. 2021, pp. 6441–6444.
- H. J. Ralston, "Energetics of Human Walking," in Neural Control of Locomotion, 1976, pp. 77–98.
- [5] J. C. Selinger, S. M. O'Connor, J. D. Wong, and J. M. Donelan, "Humans Can Continuously Optimize Energetic Cost during Walking," *Curr. Biol.*, vol. 25, no. 18, pp. 2452–2456, 2015.
- [6] M. Ackermann and A. J. van den Bogert, "Optimality principles for model-based prediction of human gait," *J. Biomech.*, vol. 43, no. 6, pp. 1055–1060, 2010.
- [7] S. Song and H. Geyer, "Predictive neuromechanical simulations indicate why walking performance declines with ageing," *J. Physiol.*, vol. 596, no. 7, pp. 1199–1210, 2018.
- [8] A. D. Koelewijn and A. J. van den Bogert, "Joint contact forces can be reduced by improving joint moment symmetry in below-knee amputee gait simulations," *Gait Posture*, vol. 49, pp. 219–225, 2016.
- [9] S. Sivakumaran, A. Schinkel-Ivy, K. Masani, and A. Mansfield, "Relationship between margin of stability and deviations in spatiotemporal gait features in healthy young adults," *Hum. Mov. Sci.*, vol. 57, no. September 2017, pp. 366–373, 2018.
- [10] M. Wu, G. Brown, and K. E. Gordon, "Control of locomotor stability in stabilizing and destabilizing environments," *Gait Posture*, vol. 55, no. April, pp. 191–198, 2017.
- [11] S. A. Antos, K. P. Kording, and K. E. Gordon, "Energy expenditure does not explain step length-width choices during walking," bioRxiv, 2021.
- [12] R. H. Miller, B. R. Umberger, J. Hamill, and G. E. Caldwell, "Evaluation of the minimum energy hypothesis and other potential optimality criteria for human running," *Proc. R. Soc. B Biol. Sci.*, vol. 279, no. 1733, pp. 1498–1505, 2012.
- [13] K. Veerkamp et al., "Evaluating cost function criteria in predicting healthy gait," J. Biomech., vol. 123, p. 110530, 2021.
- [14] A. Falisse, G. Serrancolí, C. L. Dembia, J. Gillis, I. Jonkers, and F. De Groote, "Rapid predictive simulations with complex musculoskeletal models suggest that diverse healthy and pathological human gaits can emerge from similar control strategies," J. R. Soc. Interface, vol. 16, no. 157, Aug. 2019.
- [15] T. W. Dorn, J. M. Wang, J. L. Hicks, and S. L. Delp, "Predictive simulation generates human adaptations during loaded and inclined walking," *PLoS One*, vol. 10, no. 4, pp. 1–16, 2015.
- [16] W. Li and N. P. Fey, "Neuromechanical Control Strategies of Frontal-Plane Angular Momentum of Human Upper Body During Locomotor Transitions," in 2018 7th IEEE International Conference on Biomedical Robotics and Biomechatronics (Biorob), Aug. 2018, vol. 2018-Augus, pp. 984–989.
- [17] A. Seth et al., "OpenSim: Simulating musculoskeletal dynamics and neuromuscular control to study human and animal movement.," PLoS Comput. Biol., vol. 14, no. 7, p. e1006223, 2018.
- [18] S. L. Delp, J. P. Loan, M. G. Hoy, F. E. Zajac, E. L. Topp, and J. M. Rosen, "An Interactive Graphics-Based Model of the Lower Extremity to Study Orthopaedic Surgical Procedures," *IEEE Transactions on Biomedical Engineering*, vol. 37, no. 8, pp. 757–767, 1990.
- [19] W. Li and N. P. Fey, "A Predictive Framework to Provide Neuromuscular Insights in Reshaping Dynamic Balance during Transient Locomotion," in 2021 43rd Annual International Conference of the IEEE Engineering in Medicine & Biology Society (EMBC), Nov. 2021, pp. 4812–4815.
- [20] S. Porsa, Y.-C. Lin, and M. G. Pandy, "Direct Methods for Predicting Movement Biomechanics Based Upon Optimal Control Theory with Implementation in OpenSim," *Ann. Biomed. Eng.*, vol. 44, no. 8, pp. 2542–2557, 2016.
- [21] G. Serrancoli et al., "Subject-Exoskeleton Contact Model Calibration Leads to Accurate Interaction Force Predictions," *IEEE Trans. Neural Syst. Rehabil. Eng.*, vol. 27, no. 8, pp. 1597–1605, 2019.
- [22] B. R. Umberger, "Stance and swing phase costs in human walking," J. R. Soc. Interface, vol. 7, no. 50, pp. 1329–1340, 2010.
- [23] H. Herr and M. Popovic, "Angular momentum in human walking," *J. Exp. Biol.*, vol. 211, no. 4, pp. 467–481, 2008.
- [24] J. S. Frank and A. E. Patla, "Balance and mobility challenges in older adults: Implications for preserving community mobility," Am. J. Prev. Med., vol. 25, no. 3 SUPPL. 2, pp. 157–163, 2003.